

1 **The selenophosphate synthetase, *selD*, is important for *Clostridioides difficile***
2 **physiology**

3

4 Kathleen N. McAllister^{1,2}, Andrea Martinez Aguirre¹, and Joseph A. Sorg¹

5 ¹Department of Biology, Texas A&M University, College Station, TX

6 ²Present location: Skirball Institute of Biomolecular Medicine, New York University

7 School of Medicine, New York, NY

8

9 Running Title: Selenophosphate is important for *C. difficile* physiology

10

11 *Corresponding Author

12 ph: 979-845-6299

13 email: jsorg@bio.tamu.edu

14 **Abstract**

15 The endospore-forming pathogen, *Clostridioides difficile*, is the leading cause of
16 antibiotic-associated diarrhea and is a significant burden on the community and
17 healthcare. *C. difficile*, like all forms of life, incorporates selenium into proteins through a
18 selenocysteine synthesis pathway. The known selenoproteins in *C. difficile* are involved
19 in a metabolic process that uses amino acids as the sole carbon and nitrogen source
20 (Stickland metabolism). The Stickland metabolic pathway requires the use of two
21 selenium-containing reductases. In this study, we built upon our initial characterization
22 of the CRISPR-Cas9-generated *selD* mutant by creating a CRISPR-Cas9-mediated
23 restoration of the *selD* gene at the native locus. Here, we use these CRISPR-generated
24 strains to analyze the importance of selenium-containing proteins on *C. difficile*
25 physiology. SelD is the first enzyme in the pathway for selenoprotein synthesis and we
26 found that multiple aspects of *C. difficile* physiology were affected (*e.g.*, growth,
27 sporulation, and outgrowth of a vegetative cell post-spore germination). Using RNAseq,
28 we identified multiple candidate genes which likely aid the cell in overcoming the global
29 loss of selenoproteins to grow in medium which is favorable for using Stickland
30 metabolism. Our results suggest that the absence of selenophosphate (*i.e.*,
31 selenoprotein synthesis) leads to alterations to *C. difficile* physiology so that NAD⁺ can
32 be regenerated by other pathways.

33

34 **Importance**

35 *C. difficile* is a Gram-positive, anaerobic gut pathogen which infects thousands of
36 individuals each year. In order to stop the *C. difficile* lifecycle, other non-antibiotic
37 treatment options are in urgent need of development. Towards this goal, we find that a
38 metabolic process used by only a small fraction of the microbiota is important for *C.*
39 *difficile* physiology – Stickland metabolism. Here, we use our CRISPR-Cas9 system to
40 ‘knock in’ a copy of the *selD* gene into the deletion strain to restore *selD* at its native
41 locus. Our findings support the hypothesis that selenium-containing proteins are
42 important for several aspects of *C. difficile* physiology – from vegetative growth to spore
43 formation and outgrowth post-germination.

44

45 **Introduction**

46 *Clostridioides difficile* is a major concern as a nosocomial and community-
47 acquired gut pathogen (1). This pathogen has become the most common cause of
48 health care-associated infections in United States hospitals (2, 3). In 2017 in the United
49 States, approximately 223,900 cases of *C. difficile* infection were identified and nearly
50 12,800 of those resulted in death. In the same year, it was estimated that *C. difficile*
51 infections resulted in more than \$1 billion in excess health-care costs (4). The burden of
52 this pathogen on patients, the community, and health-care has led the Centers for
53 Disease Control and Prevention to identify this bacterium as an urgent threat (5).

54 Key to battling this aggressive pathogen is understanding the basic processes *C.*
55 *difficile* uses to complete its lifecycle. While our understanding of *C. difficile* physiology
56 has increased dramatically in the last decade, specifically in toxin production /

57 regulation, sporulation and germination, our understanding of metabolic processes is
58 lacking (6-11). A recent review by Neumann-Schaal *et al.* nicely discussed the known
59 metabolic processes involved in energy generation in *C. difficile* (12). *C. difficile* has
60 multiple metabolic pathways that overlap to ensure generation of key metabolites. The
61 Wood-Ljungdahl pathway was recently found to be not as active in *C. difficile* as in other
62 acetogens, but this pathway can be used in conjunction with butyrate formation to
63 regenerate NAD⁺ in the absence of Stickland metabolism (13). Carbon metabolism
64 includes breaking down sugars such as glucose and mannitol to generate pyruvate and
65 acetyl-CoA for glycolysis and the tricarboxylic acid cycle, although the latter is
66 incomplete. Pyruvate is a key metabolite in many different central carbon metabolism
67 and fermentation pathways (12). It can be utilized by pyruvate formate-lyase to generate
68 CO₂ for carbon fixation (14, 15), and it can be degraded to acetyl-CoA to generate
69 butyrate (12). Pyruvate is also used in fermentation pathways to generate propionate
70 via the reductive branch of Stickland metabolism. Fermentation pathways also include
71 Stickland metabolism which contributes to electron bifurcation and the membrane
72 spanning Rnf complex to generate a sodium/proton gradient for substrate-level
73 phosphorylation. While it appears that many of the metabolic processes in *C. difficile*
74 have been elucidated, how these processes interact when others are impaired has yet
75 to be studied (12).

76 Stickland metabolism is a primary source of energy for a small group of
77 anaerobic bacteria which use amino acids as their sole carbon and nitrogen source (*i.e.*,
78 *C. difficile*, *Clostridium sporogenes*, and *Clostridium sticklandii*). The main goal of this
79 metabolic pathway is to generate NAD⁺ and a small amount of ATP for the cell (16-19).

80 In the oxidative branch, an amino acid, most frequently isoleucine, leucine or valine
81 (ILV), is decarboxylated or deaminated and generate products for other metabolic
82 processes + NADH (17, 19, 20). In the reductive branch, D-proline or glycine are
83 deaminated or reduced by their respective reductases (proline reductase, PrdB, and
84 glycine reductase, GrdA) to regenerate NAD⁺ to be reused by the cell (17, 18, 21, 22).
85 Recently, Stickland metabolism was suggested as a significant contributor during *C.*
86 *difficile* infection in a murine model. Proline and hydroxyproline were found to be the
87 most abundant molecules at the start of infection; 5-aminovalerate, a product of the
88 proline reductase in Stickland metabolism, is an abundant molecule towards the end of
89 infection (23, 24).

90 Both the proline and glycine reductases are selenoproteins (20, 25).
91 Selenoproteins are made through the incorporation of selenium, as selenocysteine,
92 during protein synthesis. Selenocysteine is generated through a synthesis pathway
93 where inorganic phosphate reacts with hydrogen selenide to generate selenophosphate
94 by the selenophosphate synthetase, SelD. Through the use of a selenocysteinyl-tRNA
95 (Sec) synthase, SelA, selenophosphate is incorporated into serine-charged tRNAs to
96 generate selenocysteine. The selenocysteine-specific elongation factor, SelB,
97 recognizes an in-frame stop codon followed by a selenocysteine insertion sequence
98 (SECIS). This recognition results in a halt in translation to allow for the incorporation of
99 the selenocysteine into the protein sequence (26).

100 We hypothesized that if we eliminated the global production of selenoproteins,
101 the two Stickland reductases would not be generated, and the resulting strain would be
102 incapable of performing Stickland metabolism. Previously, we generated a CRISPR-

103 Cas9 genome editing tool for use in *C. difficile* (27). In that work, we created a *C.*
104 *difficile* $\Delta seID$ strain and analyzed the growth phenotype of this strain compared to the
105 wild-type parent and the mutant complemented with a wild-type *seID* allele *in trans*. We
106 showed that *C. difficile* R20291 $\Delta seID$ (KNM6) had no growth defect in rich BHIS
107 medium but did have a slight growth defect in TY medium, which is a peptide rich
108 medium and should encourage the cells to use Stickland metabolism for growth (27).
109 Here, we build upon our prior work by using the CRISPR-Cas9 system to restore the
110 *seID* gene at its native locus. Using this *seID*-restored strain, we sought to further
111 characterize this mutant throughout different lifecycles to determine the global role of
112 selenoproteins on *C. difficile* physiology. We find that loss of selenophosphate /
113 Stickland metabolism reprograms *C. difficile* metabolism to pathways that can
114 regenerate NAD⁺ from NADH.

115

116 **Results**

117 **Complementation *in trans* results in growth differences at different hydrogen** 118 **levels**

119 When originally characterizing the *C. difficile* KNM6 ($\Delta seID$) mutant strain, we
120 found that the complementing plasmid would not restore the mutant to growth
121 comparable to wild-type, in either TY or TYG medium, despite the use of a fragment
122 upstream of the *seIDAB* operon that should contain the native promoter region (Figure
123 1A). However, as published in the prior work, we were able to complement the
124 phenotype, and this complementation was dependent on the abundance of hydrogen

125 gas in the anaerobic chamber. When monitored using a COY Anaerobic Monitor (CAM-
126 12), a 4% hydrogen level did not permit the complementing plasmid to restore the
127 growth phenotype to wild-type levels (Figure 1A). However, when the hydrogen level
128 was lowered to ~1.7% we observed complementation in TY medium (Figure 1B). This
129 observation was interesting and suggests that hydrogen abundance in the anaerobic
130 chamber influences *C. difficile* physiology or the ability of *selD*, when expressed from a
131 multicopy plasmid, to function within *C. difficile*. However, to fully characterize the *C.*
132 *difficile* $\Delta selD$ mutant, we wanted to avoid this problem altogether by restoring the
133 CRISPR-Cas9-mediated deletion with *selD* at its native locus.

134 **Generation of a *C. difficile* restored *selD*⁺ strain by CRISPR-Cas9 genome editing**

135 Our previously developed tool was used to generate a $\Delta selD$ strain and was
136 limited to this type of mutation. By modifying the existing CRISPR-Cas9 plasmid, we
137 have improved the functionality of this tool to include insertions within the genome.
138 Recently, Muh *et al.* developed a *C. difficile* CRISPRi tool which included dCas9 to be
139 under the conditional expression of a xylose-inducible promoter system (28). We
140 replaced the previous tetracycline-inducible promoter system, which was shown to have
141 uncontrolled expression of Cas9, with the xylose-inducible promoter. We replaced the
142 homology region and gRNA target sequences in our new CRISPR-Cas9 gene editing
143 plasmid. The targeting region is 26 bp away from the deletion site to reintroduce *selD* at
144 its native locus (Figure 2A). Restoration-plasmid-containing *C. difficile* $\Delta selD$ was
145 passaged on xylose-containing agar medium. Using this strategy, we generated a *C.*
146 *difficile* *selD* restored strain (KNM9; $\Delta selD::selD^+$) (Figure 2B).

147 ***C. difficile* $\Delta seID$ strain has a growth defect in peptide rich medium**

148 Because we generated a *seID* restored strain, we repeated the growth
149 experiments to confirm that the restored strain would complement the phenotype. When
150 the *C. difficile* wild-type (R20291), $\Delta seID$ (KNM6), and $\Delta seID::seID^+$ (KNM9) strains
151 were grown in rich BHIS medium, we again saw no difference between the growth of
152 these three strains over 24 hours (Figure 2C). When these three strains were grown in
153 TY (Figure 2D) or TYG (Figure S1), we observed a growth defect of the $\Delta seID$ strain
154 when compared to wild-type or $\Delta seID::seID^+$ (Figures 2D and S1). Again, there was no
155 observable difference whether glucose was supplemented in the medium or not on the
156 growth of these strains. For this reason, TY medium was used for most of the
157 subsequent experiments. The growth data are consistent with our previous findings
158 along with the additional finding that the $\Delta seID$ mutant strain grows to similar levels as
159 the wild-type and restored strains in TY medium at 24 hours (Figure 2D). We will note
160 that these and all subsequent experiments were performed at ~1.7% hydrogen and will
161 discuss our rationale for this later in the manuscript.

162 **Sporulation**

163 To understand how the absence of selenoproteins impacts *C. difficile* spore
164 formation, we determined the sporulation frequency in *C. difficile* R20291, KNM6
165 ($\Delta seID$) and KNM9 ($\Delta seID::seID^+$) (29). As a negative control, we generated a deletion
166 of *spo0A* in *C. difficile* R20291 using CRISPR-Cas9 (Figure S2). When compared to the
167 *C. difficile* R20291, wild-type, strain, the *C. difficile* $\Delta seID$ mutant produced fewer spores
168 in both BHIS and TY media (Figure 3A). Restoration of the *seID* gene resulted in a

169 return of sporulation to wild-type levels. These results indicate that the absence of
170 selenoproteins / selenophosphate has a mild impact on *C. difficile* sporulation.

171 **Selenoprotein synthesis has no effect on *C. difficile* spore germination**

172 Due to the mild defect in sporulation, we then wanted to determine whether the
173 $\Delta seID$ strain had any defect in germination. Strains were grown and allowed to
174 sporulate on BHIS medium to minimize any affects from both growth and sporulation
175 defects. The spores were purified and analyzed for germination using the optical density
176 assay. When *C. difficile* wild-type (R20291), $\Delta seID$ (KNM6), and $\Delta seID::seID^+$ (KNM9)
177 spores were suspended in rich BHIS medium supplemented with 10 mM taurocholate
178 (TA), rapid germination occurred (Figure 3B). Since the mutant phenotype is apparent in
179 TY medium, we germinated spores in this medium supplemented with 10 mM TA and
180 measured the drop in optical density. Similar to rich medium, the spores rapidly
181 germinated in TY medium (Figure 3C). These results suggest that the selenophosphate
182 synthetase, *seID*, plays no significant role in the early events during spore germination.

183 **Significant delay in outgrowth of $\Delta seID$ germinated spores in peptide-rich 184 medium**

185 Because we observed a defect in growth of the *C. difficile* KNM6 ($\Delta seID$) strain,
186 we hypothesized that the strain would have a deficiency in outgrowth from spores.
187 Purified spores from wild-type *C. difficile* R20291, KNM6 ($\Delta seID$), and KNM9
188 ($\Delta seID::seID^+$) were germinated for 10 minutes at 37°C in rich BHIS medium to ensure
189 that the germination conditions would not impact outgrowth of a vegetative cell from the
190 germinated spore. After washing the germinated spores in either BHIS or TY medium,

191 the germinated spores were resuspended in the anaerobic chamber in pre-reduced
192 BHIS or TY medium. We then monitored the optical densities over a 24 hour period
193 (Figure 4). When cells were allowed to outgrow in rich BHIS medium, there was a non-
194 significant delay in growth in the *C. difficile* KNM6 ($\Delta seID$) strain of approximately thirty
195 minutes, when compared to the wild-type and restored strains (Figure 4A). On the other
196 hand, when cells were allowed to outgrow in peptide-rich, TY medium, *C. difficile* KNM6
197 ($\Delta seID$) had an observed outgrowth defect, compared to the wild-type and restored
198 strains (Figure 4B).

199 **RNA-seq comparison of wild-type versus $\Delta seID$ strains**

200 If the hypothesis that Stickland metabolism is a primary source of energy for *C.*
201 *difficile* is true, we wondered why the growth defect in peptide-rich medium was not
202 more severe compared to wild-type and restored strains. We then hypothesized that the
203 *C. difficile* KNM6 ($\Delta seID$) strain was able to compensate for the loss of global
204 selenoprotein synthesis through upregulation of other metabolic pathways. To
205 determine which pathways were differentially expressed, we performed RNA-seq on the
206 wild-type *C. difficile* R20291 and *C. difficile* KNM6 ($\Delta seID$) strains during exponential
207 growth in TY medium supplemented with glucose. At the time of performing these
208 experiments, we were not aware of whether glucose would have an effect on gene
209 expression and, therefore, decided to include this carbohydrate in the medium. We
210 performed these experiments at both ~1.7% and 4% hydrogen levels to determine
211 whether atmospheric hydrogen abundance impacts *C. difficile* physiology.

212 First, we noticed when comparing expression of genes in wild-type cells grown at
213 low and high hydrogen levels, the cells had significant down-regulation of ribosomal
214 proteins at high hydrogen. This suggests that the cells perceive high hydrogen as a
215 stressful condition. Due to this finding, we chose to exclude highly up- or down-
216 regulated gene expression due to hydrogen levels when comparing wild-type and
217 mutant expression levels. Meaning, we excluded expression of genes which had
218 significant expression changes in either low or high hydrogen levels of wild-type
219 cultures. After this exclusion, we obtained a more narrow list for comparison of wild-type
220 and $\Delta seID$ strains at low hydrogen levels and further determined their known or
221 hypothesized function and what pathway that gene belongs (Table 1) (30, 31). As
222 expected, many of the genes are involved in metabolism; 36.35% of genes which were
223 up-regulated, and 22.24% of genes which were down-regulated (Figure 5). In both
224 cases, there were large numbers of genes of unknown function, more than 25% both
225 up- and down-regulated. Other than metabolism and unknown functions, the largest
226 group which contained up-regulated expression in the $\Delta seID$ strain characterized as
227 transferases. Although, many of these genes also fit into another KEGG pathway, *i.e.*
228 metabolism. Another group of genes which was significant were those of transporters or
229 involved in secretion, likely increasing the cell's import and export systems to
230 compensate for this growth impairment. The largest group of genes which were down-
231 regulated, besides metabolism or unknown functions, belonged to secretion systems or
232 hydrolases. Again, the cell was likely increasing certain pathways or import / export
233 systems to allow energy to be utilized elsewhere.

234 **Validation of RNA-seq by quantitative RT-PCR**

235 We then chose genes which we have highlighted as well as others of interest to
236 validate the RNA-seq results by qRT-PCR. *C. difficile* R20291 and *C. difficile* KNM6
237 strains were grown as previously described for RNA-seq, DNA was depleted, and cDNA
238 libraries were generated. Using the housekeeping gene, *rpoB*, as an internal
239 normalization control, we determined the fold change of transcripts in the KNM6 (Δ *seID*)
240 strain compared to the R20291 (wild-type) strain at both 4% and 1.7% hydrogen levels.
241 The target genes *CDR20291_0962* and *CDR20291_0963* had transcript levels which
242 were interesting at 1.7% hydrogen percentage since it appeared that, in one biological
243 replicate, the riboswitch was likely turned on while other biological replicates had fold
244 change values close to one and were likely turned in the off position (Figure 6A and 6B).
245 One target gene, *mtlF*, which is part of the mannitol utilization pathway, had a slightly
246 increased fold change in transcript levels at both 4% and 1.7% by qRT-PCR, and the
247 trend correlated to the results found from RNA-seq (Figure 6C). Mannitol utilization may
248 be a large factor helping the strain grow in absence of selenoproteins.

249 Since we hypothesized Stickland metabolism to be impaired in the mutant strain,
250 we chose to analyze the proline reductase, *prdB*, and the glycine reductases, *grdB*. The
251 fold change in expression of *prdB* was higher than was seen in RNA-seq (Figure 6D). In
252 qRT-PCR, the transcription of *grdB* was down-regulated in the mutant compared to wild-
253 type (3.6- and 4.4-fold down-regulated in 4% and 1.7% hydrogen, respectively) (Figure
254 6E). On the other hand, the transcription of *grdB* was slightly up-regulated in RNA-seq
255 (1.3- and 2-fold up-regulated in 4% and 1.7% hydrogen, respectively).

256 Finally, we validated two uncharacterized genes. *CDR20291_2627*, a putative
257 hemagglutinin / adhesion, was up regulated in the RNAseq at both 4% hydrogen and

258 1.7% hydrogen. We also observed upregulation of this gene in the qRT-PCR
259 validations. Additionally, *CDR20291_2932*, a putative glutamine deaminase, was
260 slightly downregulated, and we validated this by qRT-PCR.

261 **Discussion**

262 It is becoming increasingly appreciated that Stickland metabolism and Stickland
263 substrates are important for *C. difficile* pathogenesis. In the oxidative branch of
264 Stickland metabolism, several different amino acids can be deaminated or
265 decarboxylated. In the reductive branch either proline or glycine are used by their
266 respective reductases. The proline reductase, PrdB, converts proline + NADH to 5-
267 aminovalerate + NAD⁺ while the glycine reductase, GrdA, converts glycine + NADH +
268 ADP to acetate + ATP + NAD⁺. The activity of the PrdB and GrdA proteins is dependent
269 on the incorporation of a modified amino acid, selenocysteine.

270 Incorporation of selenium into proteins is governed by the SelD, SelA and SelB
271 proteins. The first step in this pathway is the generation of selenophosphate from
272 hydrogen selenide by the selenophosphate synthetase, SelD. We hypothesized that a
273 mutation in *C. difficile selD* would significantly alter *C. difficile* physiology by blocking the
274 total incorporation of selenium into protein as an amino acid, selenocysteine, or as part
275 of selenium containing cofactors. Surprisingly, we found that plasmid-based
276 complementation of the *selD* deletion led to an odd observation – that complementation
277 only occurred at low hydrogen percentage (1.7%) in our anaerobic chamber. At higher
278 hydrogen abundance (4%), we could not complement our mutant.

279 To address this, we used our CRISPR/Cas9 genome editing tool to restore the
280 *selD* gene at its native locus. By targeting the Cas9 nuclease to a region just outside of
281 the deleted region, we were able to isolate a restored strain. This *C. difficile*
282 $\Delta selD::selD^+$ strain grew similar to the wild-type strain. We then analyzed the physiology
283 of the strains. We observed no differences in germination between the wild-type, mutant
284 and restored strains, but the $\Delta selD$ strain had a mild decrease in spore formation.
285 However, we observed a significant delay during the outgrowth of germinated *C. difficile*
286 spores in peptide-rich medium (TY). This highlights the importance of selenophosphate
287 during the early stages of return to vegetative growth.

288 To understand the overall impact of SelD on *C. difficile* physiology, we
289 determined the global expression differences between the wild-type and mutant strains
290 at low and high hydrogen percentages. First, we observed that *fdhA* was upregulated in
291 the *selD* mutant strain. *fdhA* encodes the selenocysteinyl-tRNA synthetase that charges
292 serine charged tRNA with selenophosphate to generate selenocysteine-charged tRNA.
293 This suggests that in the absence of selenoprotein, *C. difficile* senses this loss and
294 attempts to increase the rate of selenocysteine-charged tRNA.

295 On first glance, *CDR20291_0963* and *CDR20291_0962* are the two most highly
296 up-regulated genes in the $\Delta selD$ strain. *CDR20291_0963* is uncharacterized in *C.*
297 *difficile* but has high similarity to the AlgI protein, an alginate O-acetyltransferase,
298 characterized in *Pseudomonas aeruginosa*. Whether this protein has the same function
299 in *C. difficile* is yet to be determined. The other gene *CDR20291_0962* is an
300 uncharacterized gene of no known function. When ran through NCBI BLAST and the
301 Conserved Domain Database (32, 33), this protein sequence has a DHHW domain

302 which is common among bacteria. What we found interesting is that both of these genes
303 have recently been characterized to contain a riboswitch upstream, and their altered
304 expression is likely unrelated to the *seID* mutation but, rather, due to the riboswitch
305 being in the “ON” position (34).

306 Interestingly, every gene in the operon *mtIARFD* had upregulated expression in
307 the $\Delta seID$ strain. The expression levels varied between almost 3- to 5-fold up-regulation
308 compared to wild-type. We hypothesize that mannose metabolism may play a larger
309 role in a strain lacking selenoproteins. In this pathway, mannitol is taken into the cell
310 and broken down to mannitol-1-phosphate by MtlF and MtlA. Then, MtlD uses NAD^+ to
311 convert mannitol-1-phosphate into fructose-6-phosphate + $NADH$ to then be used for
312 glycolysis (35-38). Prior work by Teschner and Garel (1990) has shown that the *E. coli*
313 MtlD can run this reaction in reverse to generate NAD^+ instead of consuming it (39).

314 Besides mannose metabolism, cysteine and methionine metabolism appeared to
315 be increased by the up-regulation of *cysM* and *cysA*. It is interesting that these genes
316 are utilizing H_2S produced by *C. difficile* to generate L-cysteine and acetate (40, 41).
317 Acetate is also a final product in the reduction of glycine by Stickland metabolism (17). It
318 is possible that the cell is generating acetate through this method in order to utilize the
319 molecule in other metabolic pathways.

320 Another metabolic process which had multiple genes up-regulated was for
321 riboflavin synthesis: *ribD*, a deaminase and reductase; *ribH*, a lumazine synthase; and
322 *ribB*, a riboflavin synthase. Riboflavin is an essential cofactor which can be broken down
323 into flavins (flavin mononucleotide, FMNs) and flavin adenine dinucleotide (FAD) to be

324 used by the cell. Riboflavin can also be taken up by the environment if present (42). A
325 gene proposed to be a riboflavin transporter, *CDR20291_0146*, was also up-regulated
326 from our RNA-seq analysis. This essential cofactor is likely being used in multiple
327 processes and its synthesis or uptake is being up-regulated to feed these metabolic
328 pathways.

329 Of those genes which had down-regulated expression, there are a few worth
330 noting. Multiple genes involved in transport or utilization of amino acids were down-
331 regulated, possible due to the decrease in the dependence on Stickland metabolism to
332 provide NAD⁺ for the cell to generate energy. *CDR20291_2931*, a putative amino acid
333 permease for transport of amino acids into the cell, and *CDR20291_2932*, a putative
334 glutamine amidotransferase for transforming glutamine into generating an available
335 carbon-nitrogen group, both are proposed to be involved in the utilization of amino acids
336 (43, 44). As well, a putative sodium:dicarboxylate symporter, *CDR20291_2077*, could
337 also be involved in amino acid uptake into the cell. The down-regulation of these three
338 genes indicates that the cell is moving its resources away from the degradation of
339 amino acids as a source of energy.

340 Overall, our data highlight the importance of selenophosphate for *C. difficile*
341 physiology. The absence of selenophosphate leads to the rerouting of *C. difficile*
342 metabolism so that the cell is less dependent on Stickland metabolism of amino acids
343 and the regeneration of NAD⁺ by the reductive branch of Stickland. However, what was
344 surprising was the impact of atmospheric chamber conditions (H₂ percentage) on *C.*
345 *difficile* physiology. Further work should be done to understand how hydrogen
346 abundance influences *C. difficile* physiology, potentially in autotrophic metabolism, and

347 when reporting on *C. difficile* physiology the concentration of hydrogen should be
348 reported.

349

350 **Materials and Methods**

351 **Bacterial strains and growth conditions**

352 *C. difficile* strains were routinely grown in an anaerobic atmosphere (1.7% - 4%
353 H₂, 5% CO₂, 85% N₂) at 37°C in brain heart infusion supplemented with 5 g / L yeast
354 extract and 0.1% L-cysteine (BHIS), as described previously (8, 45-47), or TY media
355 (3% tryptone, 2% yeast extract) (48). Hydrogen levels were determined by a COY
356 Anaerobic Monitor (CAM-12). For conjugation experiments, cells were plated on TY
357 medium for *Bacillus subtilis*-based conjugations. Where indicated, growth was
358 supplemented with taurocholate (TA; 0.1% w / v), thiamphenicol (10 µg / mL), D-
359 cycloserine (250 µg / mL), xylose (1% w / v) and / or glucose (1% w / v) as needed.
360 Induction of the CRISPR-Cas9 system was performed on TY agar plates supplemented
361 with thiamphenicol (10 µg / mL) and xylose (1% w / v). *E. coli* strains were routinely
362 grown at 37°C in LB medium. Strains were supplemented with chloramphenicol (20 µg /
363 mL) as needed. *B. subtilis* BS49 was routinely grown at 37°C in LB broth or on LB agar
364 plates. Strains were supplemented with chloramphenicol (2.5 µg / mL) and/or
365 tetracycline (5 µg / mL).

366 **Plasmid construction and molecular biology**

367 To construct the CRISPR-Cas9 *selD* complementing plasmid, the previously
368 published CRISPR-Cas9 *pyrE* targeting plasmid, pJK02 (27), was modified by replacing
369 *traJ* with oriT *tn916* for *B. subtilis* conjugation by amplification from pJS116 using
370 primers 5'Tn916ori and 3'Tn916ori. The resulting fragments was introduced into pJK02
371 by Gibson assembly at the *Apal* site and transformed into *E. coli* DH5 α to generate
372 pKM126. Next, the donor region to be used for homology directed repair was PCR
373 amplified from *C. difficile* R20291 genomic DNA using primers 5'selD_comp and
374 3'selD_comp 2 where this fragment contains a 500 bp upstream homology arm and a
375 500 bp downstream homology arm surrounding *selD*. The resulting fragment was
376 cloned by Gibson assembly into pKM126 at the *NotI* and *XhoI* restriction sites and
377 transformed into *E. coli* DH5 α to generate pKM181. Lastly, the gBlock for *selD* targeting
378 sgRNA, CRISPR_selD_comp2, was introduced by Gibson assembly into the *KpnI* and
379 *MluI* restriction sites and transformed into *E. coli* DH5 α resulting in pKM183. To improve
380 efficiency of the CRISPR-Cas9 editing system and provide more control of Cas9
381 expression, the tetracycline-inducible system was replaced with the xylose inducible
382 system (28). To do this, the xylose inducible promoter was PCR amplified from pIA33
383 using primers 5'selDcomp_HR_xylR 2 and 3'cas9_Pxyl 2 and inserted by Gibson
384 assembly into pKM183 at the *XhoI* and *PacI* restriction sites and transformed into *E. coli*
385 DH5 α to generate pKM194.

386 To construct the CRISPR-Cas9 *spo0A* deletion mutant, the gBlock for *spo0A*
387 targeting sgRNA, CRISPR_spo0A_2, was introduced by Gibson assembly into the *KpnI*
388 and *MluI* restriction sites in pKM197 (49) and transformed into *E. coli* DH5 α resulting in
389 pKM213. The homology arms to be used for homology directed repair was PCR

390 amplified from *C. difficile* R20291 genomic DNA using primers 5'spo0A_UP and
391 3'spo0A_UP for the 500 bp upstream arm and primers 5'spo0A_DN and 3'spo0A_DN
392 for the 500 bp downstream arm. The resulting fragments were then cloned by Gibson
393 assembly at the *NotI* and *XhoI* restriction sites and transformed into *E. coli* DH5 α
394 resulting in pKM215.

395 **Conjugation for CRISPR-Cas9 plasmid insertion**

396 CRISPR-Cas9 plasmid pKM194 was transformed into *B. subtilis* BS49 to be used
397 as a donor for conjugation with *C. difficile* KNM6. Likewise, the pKM215 plasmid was
398 transformed into *B. subtilis* BS49 to be used as a donor for conjugation with *C. difficile*
399 R20291. *C. difficile* R20291 or KNM6 was grown anaerobically in BHIS broth overnight.
400 This was then diluted in fresh pre-reduced BHIS broth and grown anaerobically for 4
401 hours. Meanwhile, *B. subtilis* BS49 containing the CRISPR plasmids were grown
402 aerobically at 37°C in LB broth supplemented with tetracycline and chloramphenicol for
403 3 hours. One hundred microliters of each culture was pated on TY agar medium. After
404 24 hours, the growth was harvested by suspending in 2 mL pre-reduced BHIS broth. A
405 loopful of this suspended growth was spread onto several BHIS agar plates
406 supplemented with thiamphenicol, kanamycin, and D-cycloserine. *C. difficile*
407 transconjugants were screened for the presence of Tn916 using tetracycline resistance,
408 as described previously. Thiamphenicol-resistant, tetracycline-sensitive transconjugants
409 were selected and used for further experiments.

410 **Induction of the CRISPR-Cas9 system and isolating mutants**

411 The *C. difficile* KNM6 strain containing the *selD*-targeting plasmid, pKM194, was
412 streaked onto TY agar medium supplemented with thiamphenicol and xylose for
413 induction. This was then passaged a second time on the same medium. After isolating
414 colonies on BHIS supplemented with xylose, DNA was extracted and tested for the
415 insertion by PCR amplification of the *selD* region using primers 5'*selD* and 3'*selD*. From
416 this, one mixed colony out of 12 samples was isolated. This mixed colony was then
417 passaged on TY agar medium supplemented with thiamphenicol and xylose. Colonies
418 were isolated on BHIS agar medium supplemented with xylose, DNA was extracted,
419 and isolates were tested by PCR amplification again as above. From this, 14 colonies
420 were insertions out of 15. Confirmed restored strains were passaged 3 times in BHIS
421 liquid medium in order to lose the CRISPR-Cas9 plasmid. After pick-and-patch on BHIS
422 agar with and without thiamphenicol, loss of plasmid was confirmed by PCR
423 amplification of a portion of *cas9* using primer set 5'*tetR_CO_Cas9* and 3'*COcas9* (975)
424 and the *gRNA* using primer set 5'*gdh* and 3'*gRNA 2*.

425 The *C. difficile* R20291 strain containing the *spo0A*-targeting plasmid, pKM215,
426 was streaked onto TY agar medium supplemented with thiamphenicol and xylose for
427 induction. This was then passaged a second time on the same medium. After isolating
428 colonies on BHIS supplemented with xylose, DNA was extracted and tested for the
429 insertion by PCR amplification of the *spo0A* region using primers 5'*spo0A_del* and
430 3'*spo0A_del*. All tested colonies (36 total) were mutants. Two isolates were passaged
431 twice in BHIS liquid medium in order to lose the CRISPR-Cas9 plasmid. After pick-and-
432 patch on BHIS agar with and without thiamphenicol, loss of plasmid was confirmed by

433 PCR amplification of a portion of *cas9* using primer set 5'tetR_CO_Cas9 and 3'COcas9
434 (975) and the gRNA using primer set 5'gdh and 3'gRNA 2.

435 **Sporulation and heat resistance assay**

436 To determine differences in sporulation efficiencies between the *C. difficile*
437 R20291 (wild-type), KNM6 ($\Delta seID$), KNM9 ($\Delta seID::seID^+$) and KNM10 ($\Delta spo0A$) strains,
438 sporulation and heat resistance was determined as described previously (29). Briefly, *C.*
439 *difficile* R20291, KNM6, KNM9, and KNM10 strains were spread onto BHIS agar
440 medium supplemented with taurocholate. From this, colonies were restreaked onto
441 either BHIS or TY agar media, making a lawn on the plate. After 48 hours of growth, half
442 of the plate was harvested and mixed into 600 μ L of pre-reduced PBS. Then, 300 μ L of
443 the sample was transferred to a separate tube and heat treated at 65°C in a heat block
444 for 30 minutes, inverting the tube every 10 minutes to ensure even heating. Both the
445 untreated and the heat-treated samples were serially diluted in PBS and plated onto
446 BHIS agar medium supplemented with taurocholate. CFUs were counted 22 hours after
447 plating. Heat resistance was calculated by dividing the CFUs for the heat-treated
448 sample by the CFUs for the untreated sample, and the average was calculated for each
449 strain.

450 **Spore purification**

451 Spores were purified from *C. difficile* R20291, KNM6, and KNM9 strains as
452 previously described (46, 50, 51). Briefly, spores were streaked onto BHIS agar medium
453 (20 – 30 plates) and allowed to sporulate for 5 to 6 days before scraping each into
454 microcentrifuge tubes containing 1 mL of sterile dH₂O and kept at 4 °C overnight. The

455 spores and debris mixture was washed five times in sterile dH₂O by centrifuging for 1
456 minute at 14,000 x g per wash. Spores were combined into 2 mL aliquots in sterile
457 dH₂O and layered on top of 8 mL of 50% sucrose and centrifuged at 4,000 x g for 20
458 minutes. The supernatant containing vegetative cells and cell debris was discarded and
459 the spores were resuspended in sterile dH₂O and washed five more times as before.
460 The spores were stored at 4 °C until use.

461 **Germination assay**

462 Purified *C. difficile* R20291, KNM6, and KNM9 spores were first heat activated at
463 65°C for 30 minutes and then placed on ice until use. To compare germination between
464 the three strains, the OD₆₀₀ was measured over time in different media. Germination
465 was carried out in clear Falcon 96-well plates at 37 °C in a final volume of 100 µL and
466 final concentrations of 10 mM taurocholate and 1X BHIS or TY. Spores were added to a
467 final OD₆₀₀ of 0.5 and germination was analyzed for 1 hour using a plate reader
468 (Spectramax M3 Plate Reader, Molecular Devices, Sunnyvale, CA) (50, 52).

469 **Outgrowth assays**

470 Purified *C. difficile* R20291, KNM6, and KNM9 spores were heat activated at
471 65°C for 30 minutes and then placed on ice until use. Spore samples were washed one
472 time with dH₂O and then added spores to a final optical density (OD₆₀₀) of 0.5 in 8 mL of
473 BHIS medium supplemented with taurocholate (10 mM final concentration). Incubated
474 the spores in germination solution in a hot water bath at 37 °C for 10 minutes and then
475 immediately placed on ice. In all subsequent steps, the germinated spores were kept on
476 ice or at 4°C. Washed once with BHIS or TY medium and removed supernatant. The

477 germinated spores were passed into the anaerobic chamber without using vacuum
478 (flooded chamber with gas) and resuspended each in 20 mL of pre-reduced BHIS or TY
479 medium. The outgrowth was monitored by measuring OD₆₀₀ over time.

480 **RNA processing**

481 *C. difficile* R20291 (wild-type) and KNM6 (Δ *seID*) was grown to an OD₆₀₀ of 0.6 in
482 TYG medium at low (1.7%) and high (4%) hydrogen levels. At that time, RNA was
483 extracted as described using the FastRNA Blue Kit (MP Biologicals). DNA was depleted
484 using the TURBO DNA-free kit (Invitrogen), repeating the steps in the kit three times to
485 achieve complete depletion. rRNA was then depleted using the Ribo-Zero rRNA
486 Removal kit for bacteria (Illumina). Enrichment of mRNA and generation of cDNA
487 libraries were completed using the TruSeq Stranded mRNA library prep kit (Illumina).

488 **RNA-seq**

489 cDNA libraries were submitted for Illumina high output single-end 50 sequencing
490 at the Tufts Genomic Core. Reads were assembled using the DNASTAR SeqMan
491 NGen 15 program in a combined assembly noting replicates. Raw expression data
492 between wild-type and mutant strains was then normalized to *rpoB* and then quantified
493 Using DNASTAR ArrayStar 15, assemblies were normalized by assigned Reads Per
494 Kilobase of template per Million mapped reads (RPKM), experiments' values were
495 capped at a minimum of 1, and all genes were normalized by calibration to the median
496 expression value of *rpoB*. Fold-change was determined four ways: wild-type at 4%
497 hydrogen to wild-type at 1.7% hydrogen, wild-type at 1.7% to wild-type at 4%, wild-type
498 at 4% to mutant at 4%, and wild-type at 1.7% to mutant at 1.7%. Expression which was

499 > 2-fold up- or down-regulated from comparison of wild-type at the different hydrogen
500 levels was excluded when comparing the respective wild-type to mutant comparisons.
501 From this, any gene expression which was > 2-fold up- or down-regulated was
502 considered significant. As a final step, we excluded any genes which had little coverage
503 or low reads visualized using DNASTAR GenVision.

504 **Quantitative RT-PCR**

505 *C. difficile* R20291 (wild-type) and KNM6 (Δ *selD*) was grown, RNA was
506 extracted, and DNA was depleted the same as described above. 50 ng of total RNA
507 was used in cDNA synthesis using the SuperScript III First-Strand Synthesis System
508 (Thermo Scientific) according to the protocol, including controls for each sample without
509 the presence of reverse transcriptase. Primer to be used for quantitative reverse
510 transcription-PCR (qRT-PCR) were designed using the Primer Express 3.0 software
511 (Applied Biosystems) and efficiencies were validated prior to use. cDNA samples were
512 then used as templates for qPCR reactions to amplify *CDR20291_0963*,
513 *CDR20291_0962*, *prdB*, *grdB*, *mtlF*, *CDR20291_2627*, and *CDR20291_2932* (primers
514 are listed in Supplemental Table 3) using PowerUp SYBR Green Master Mix (Applied
515 Biosystems) and a QuantStudio 6 Flex Real-Time PCR machine (Applied Biosystems).
516 Reactions were performed in a final volume of 10 μ L including 1 μ L undiluted cDNA
517 sample and 500 nM of each primer. Reactions were ran in technical triplicate of each
518 biological triplicate for both wild-type and mutant samples at each hydrogen level.
519 Outliers of technical replicate samples were omitted from analysis. Results were
520 calculated using the comparative cycle threshold method (53), in which the amount of
521 target mRNA was normalized to that of an internal control (*rpoB*).

522 **Statistical Analysis**

523 *C. difficile* R20291 pJS116 (wild-type, empty vector), *C. difficile* KNM6 pJS116
524 ($\Delta selD$, empty vector), and *C. difficile* KNM9 ($\Delta selD::selD^+$, $p selD$) strains were grown in
525 biological duplicate. *C. difficile* R20291, KNM6, and KNM9 strains were grown in
526 biological triplicate. *C. difficile* R20291, KNM6, KNM9, and KNM10 strains were allowed
527 to sporulate in biological triplicate. *C. difficile* R20291, KNM6, and KNM9 spores were
528 purified in biological triplicate where each replicate was grown / sporulated and purified
529 separately to be used for germination and outgrowth assays. RNA was extracted from
530 *C. difficile* R20291 and KNM6 strains for RNA-seq in biological duplicate for each strain.
531 RNA was extracted from *C. difficile* R20291 and KNM6 strains for qRT-PCR in
532 biological triplicate and each was run in technical triplicate as well. In each experiment,
533 data represents averages of each of the indicated replicates and error bars represent
534 the standard deviation from the mean. Technical replicate outliers were excluded from
535 qRT-PCR analysis.

536

537 **Acknowledgments**

538 We would like to thank Dr. Craig Ellermeier at the University of Iowa for the
539 generous gift of the xylose inducible promoter. We would also like to thank members of
540 the Sorg lab, Dr. Leif Smith, and members from Dr. Leif Smith's lab at Texas A&M
541 University for their helpful comments and suggestions during the preparation of this
542 manuscript.

543 This project was supported by awards 5R01AI116895 and 1U01AI124290 to
544 J.A.S. from the National Institute of Allergy and Infectious Diseases. The content is
545 solely the responsibility of the authors and does not necessarily represent the official
546 views of the NIAID. The funders had no role in study design, data collection and
547 interpretation, or the decision to submit the work for publication.

548

549 References

- 550 1. **Poutanen SM, Simor AE.** 2004. *Clostridium difficile*-associated diarrhea in adults.
551 CMAJ **171**:51-58.
- 552 2. **Rupnik M, Wilcox MH, Gerding DN.** 2009. *Clostridium difficile* infection: new
553 developments in epidemiology and pathogenesis. Nat Rev Microbiol **7**:526-536.
- 554 3. **Smits WK, Lyras D, Lacy DB, Wilcox MH, Kuijper EJ.** 2016. *Clostridium difficile*
555 infection. Nat Rev Dis Primers **2**:16020.
- 556 4. **CDC.** 2019. Antibiotic Resistance Threats in the United States, 2019. U.S. Department
557 of Health and Human Services, CDC.
- 558 5. **Voth DE, Ballard JD.** 2005. *Clostridium difficile* toxins: mechanism of action and role in
559 disease. Clin Microbiol Rev **18**:247-263.
- 560 6. **Lyras D, O'Connor JR, Howarth PM, Sambol SP, Carter GP, Phumoonna T, Poon R,
561 Adams V, Vedantam G, Johnson S, Gerding DN, Rood JI.** 2009. Toxin B is essential
562 for virulence of *Clostridium difficile*. Nature **458**:1176-1179.
- 563 7. **Kuehne SA, Cartman ST, Heap JT, Kelly ML, Cockayne A, Minton NP.** 2010. The
564 role of toxin A and toxin B in *Clostridium difficile* infection. Nature **467**:711-713.
- 565 8. **Francis MB, Allen CA, Shrestha R, Sorg JA.** 2013. Bile acid recognition by the
566 *Clostridium difficile* germinant receptor, CspC, is important for establishing infection.
567 PLoS Pathog **9**:e1003356.
- 568 9. **Dineen SS, Villapakkam AC, Nordmant JT, Sonenshein AL.** 2007. Repression of
569 *Clostridium difficile* toxin gene expression by CodY. Molecular Microbiology **61**:1335-
570 1351.
- 571 10. **Dembek M, Barquist L, Boinett CJ, Cain AK, Mayho M, Lawley TD, Fairweather NF,
572 Fagan RP.** 2015. High-throughput analysis of gene essentiality and sporulation in
573 *Clostridium difficile*. MBio **6**:e02383.
- 574 11. **Fimlaid KA, Bond JP, Schutz KC, Putnam EE, Leung JM, Lawley TD, Shen A.** 2013.
575 Global analysis of the sporulation pathway of *Clostridium difficile*. PLoS Genet
576 **9**:e1003660.
- 577 12. **Neumann-Schaal M, Jahn D, Schmidt-Hohagen K.** 2019. Metabolism the Difficile way:
578 The key to the success of the pathogen *Clostridioides difficile*. Front Microbiol **10**:219.
- 579 13. **Gencic S, Grahame DA.** 2020. Diverse energy-conserving pathways in *Clostridium*
580 *difficile*: Growth in the absence of amino acid Stickland acceptors and the role of the
581 Wood-Ljungdahl pathway. J Bacteriol **202**.

- 582 14. **Pinske C, Sawers RG.** 2016. Anaerobic formate and hydrogen metabolism. *EcoSal*
583 Plus 7.
- 584 15. **Ragsdale SW.** 1997. The eastern and western branches of the Wood/Ljungdahl
585 pathway: how the east and west were won. *Biofactors* 6:3-11.
- 586 16. **Nisman B, Raynaud M, Cohen GN.** 1948. Extension of the Stickland reaction to several
587 bacterial species. *Arch Biochem* 16:473.
- 588 17. **Stickland LH.** 1935. Studies in the metabolism of the strict anaerobes (genus
589 *Clostridium*): The oxidation of alanine by *Cl. sporogenes*. IV. The reduction of glycine by
590 *Cl. sporogenes*. *The Biochemical journal* 29:889-898.
- 591 18. **Stickland LH.** 1935. Studies in the metabolism of the strict anaerobes (Genus
592 *Clostridium*): The reduction of proline by *Cl. sporogenes*. *The Biochemical journal*
593 29:288-290.
- 594 19. **Stickland LH.** 1934. Studies in the metabolism of the strict anaerobes (genus
595 *Clostridium*): The chemical reactions by which *Cl. sporogenes* obtains its energy. *The*
596 *Biochemical journal* 28:1746-1759.
- 597 20. **Bouillaut L, Self WT, Sonenshein AL.** 2013. Proline-dependent regulation of
598 *Clostridium difficile* Stickland metabolism. *J Bacteriol* 195:844-854.
- 599 21. **Stadtman TC.** 1956. Studies on the enzymic reduction of amino acids: a proline
600 reductase of an amino acid-fermenting *Clostridium*, strain HF. *The Biochemical journal*
601 62:614-621.
- 602 22. **Stadtman TC, Elliott P.** 1957. Studies on the enzymic reduction of amino acids. II.
603 Purification and properties of D-proline reductase and a proline racemase from
604 *Clostridium sticklandii*. *J Biol Chem* 228:983-997.
- 605 23. **Jenior ML, Leslie JL, Young VB, Schloss PD.** 2017. *Clostridium difficile* colonizes
606 alternative nutrient niches during infection across distinct murine gut microbiomes.
607 *mSystems* 2.
- 608 24. **Jenior ML, Leslie JL, Young VB, Schloss PD.** 2018. *Clostridium difficile* alters the
609 structure and metabolism of distinct cecal microbiomes during initial infection to promote
610 sustained colonization. *mSphere* 3.
- 611 25. **Jackson S, Calos M, Myers A, Self WT.** 2006. Analysis of proline reduction in the
612 nosocomial pathogen *Clostridium difficile*. *Journal of Bacteriology* 188:8487-8495.
- 613 26. **Self WT.** 2010. Specific and nonspecific incorporation of selenium into macromolecules.
614 *Comprehensive Natural Products II: Chemistry and Biology, Vol 5: Amino Acids,*
615 *Peptides and Proteins*:121-148.
- 616 27. **McAllister KN, Bouillaut L, Kahn JN, Self WT, Sorg JA.** 2017. Using CRISPR-Cas9-
617 mediated genome editing to generate *C. difficile* mutants defective in selenoproteins
618 synthesis. *Scientific Reports* 7:14672.
- 619 28. **Muh U, Pannullo AG, Weiss DS, Ellermeier CD.** 2019. A xylose-inducible expression
620 system and a CRISPRi-plasmid for targeted knock-down of gene expression in
621 *Clostridioides difficile*. *J Bacteriol*.
- 622 29. **Shen A, Fimlaid KA, Pishdadian K.** 2016. Inducing and quantifying *Clostridium difficile*
623 spore formation. *Methods in molecular biology* 1476:129-142.
- 624 30. **Kanehisa M, Goto S.** 2000. KEGG: kyoto encyclopedia of genes and genomes. *Nucleic*
625 *Acids Res* 28:27-30.
- 626 31. **Kanehisa M, Sato Y, Kawashima M, Furumichi M, Tanabe M.** 2016. KEGG as a
627 reference resource for gene and protein annotation. *Nucleic Acids Res* 44:D457-462.
- 628 32. **Marchler-Bauer A, Bo Y, Han L, He J, Lanczycki CJ, Lu S, Chitsaz F, Derbyshire**
629 **MK, Geer RC, Gonzales NR, Gwadz M, Hurwitz DI, Lu F, Marchler GH, Song JS,**
630 **Thanki N, Wang Z, Yamashita RA, Zhang D, Zheng C, Geer LY, Bryant SH.** 2017.
631 CDD/SPARCLE: functional classification of proteins via subfamily domain architectures.
632 *Nucleic Acids Res* 45:D200-D203.

- 633 33. **Altschul SF, Gish W, Miller W, Myers EW, Lipman DJ.** 1990. Basic local alignment
634 search tool. *J Mol Biol* **215**:403-410.
- 635 34. **Sekulovic O, Mathias Garrett E, Bourgeois J, Tamayo R, Shen A, Camilli A.** 2018.
636 Genome-wide detection of conservative site-specific recombination in bacteria. *PLoS*
637 *Genet* **14**:e1007332.
- 638 35. **Behrens S, Mitchell W, Bahl H.** 2001. Molecular analysis of the mannitol operon of
639 *Clostridium acetobutylicum* encoding a phosphotransferase system and a putative PTS-
640 modulated regulator. *Microbiology (Reading)* **147**:75-86.
- 641 36. **Watanabe S, Hamano M, Kakeshita H, Bunai K, Tojo S, Yamaguchi H, Fujita Y,**
642 **Wong SL, Yamane K.** 2003. Mannitol-1-phosphate dehydrogenase (MtlD) is required
643 for mannitol and glucitol assimilation in *Bacillus subtilis*: possible cooperation of mtl and
644 gut operons. *J Bacteriol* **185**:4816-4824.
- 645 37. **Zhang M, Gu L, Cheng C, Ma J, Xin F, Liu J, Wu H, Jiang M.** 2018. Recent advances
646 in microbial production of mannitol: utilization of low-cost substrates, strain development
647 and regulation strategies. *World J Microbiol Biotechnol* **34**:41.
- 648 38. **Byer T, Wang J, Zhang MG, Vather N, Blachman A, Visser B, Liu JM.** 2017. MtlR
649 negatively regulates mannitol utilization by *Vibrio cholerae*. *Microbiology (Reading)*
650 **163**:1902-1911.
- 651 39. **Teschner W, Serre MC, Garel JR.** 1990. Enzymatic properties, renaturation and
652 metabolic role of mannitol-1-phosphate dehydrogenase from *Escherichia coli*. *Biochimie*
653 **72**:33-40.
- 654 40. **Pye VE, Tingey AP, Robson RL, Moody PC.** 2004. The structure and mechanism of
655 serine acetyltransferase from *Escherichia coli*. *J Biol Chem* **279**:40729-40736.
- 656 41. **Rabeh WM, Cook PF.** 2004. Structure and mechanism of O-acetylserine sulfhydrylase.
657 *J Biol Chem* **279**:26803-26806.
- 658 42. **Vitreschak AG, Rodionov DA, Mironov AA, Gelfand MS.** 2002. Regulation of
659 riboflavin biosynthesis and transport genes in bacteria by transcriptional and
660 translational attenuation. *Nucleic Acids Res* **30**:3141-3151.
- 661 43. **Mantsala P, Zalkin H.** 1984. Glutamine nucleotide sequence of *Saccharomyces*
662 *cerevisiae* ADE4 encoding phosphoribosylpyrophosphate amidotransferase. *J Biol*
663 *Chem* **259**:8478-8484.
- 664 44. **Massiere F, Badet-Denisot MA.** 1998. The mechanism of glutamine-dependent
665 amidotransferases. *Cellular and molecular life sciences : CMLS* **54**:205-222.
- 666 45. **Allen CA, Babakhani F, Sears P, Nguyen L, Sorg JA.** 2013. Both fidaxomicin and
667 vancomycin inhibit outgrowth of *Clostridium difficile* spores. *Antimicrob Agents*
668 *Chemother* **57**:664-667.
- 669 46. **Francis MB, Allen CA, Sorg JA.** 2015. Spore cortex hydrolysis precedes dipicolinic
670 acid release during *Clostridium difficile* spore germination. *J Bacteriol* **197**:2276-2283.
- 671 47. **Sorg JA, Dineen SS.** 2009. Laboratory maintenance of *Clostridium difficile*. *Curr Protoc*
672 *Microbiol* **Chapter 9**:Unit9A 1.
- 673 48. **Dupuy B, Sonenshein AL.** 1998. Regulated transcription of *Clostridium difficile* toxin
674 genes. *Mol Microbiol* **27**:107-120.
- 675 49. **Bhattacharjee D, Sorg JA.** 2020. Factors and conditions that impact electroporation of
676 *Clostridioides difficile* strains. *mSphere* **5**.
- 677 50. **Shrestha R, Cochran AM, Sorg JA.** 2019. The requirement for co-germinants during
678 *Clostridium difficile* spore germination is influenced by mutations in *yabG* and *cspA*.
679 *PLoS Pathog* **15**:e1007681.
- 680 51. **Francis MB, Sorg JA.** 2016. Detecting cortex fragments during bacterial spore
681 germination. *J Vis Exp*.
- 682 52. **Shrestha R, Sorg JA.** 2018. Hierarchical recognition of amino acid co-germinants
683 during *Clostridioides difficile* spore germination. *Anaerobe* **49**:41-47.

684 53. **Schmittgen TD, Livak KJ.** 2008. Analyzing real-time PCR data by the comparative C(T)
685 method. Nature protocols **3**:1101-1108.

686

687 **Tables**

688

689 **Table 1: Differentially expressed genes in the *C. difficile* Δ *selD* strain compared to**
690 **the wild-type strain.**

Name	Fold-change	Annotation/KEGG function	KEGG pathway
Up-regulated			
<i>CDR20291_0963</i>	70.544	alginate O-acetyl transferase complex protein	Unclassified Metabolism
<i>CDR20291_0962</i>	44.982	putative uncharacterized protein	Unknown
<i>CDR20291_0440</i>	17.707	cell surface protein (putative hemagglutinin / adhesin)	Unknown
<i>CDR20291_1747</i>	12.712	putative conjugative transposon regulatory protein	Unknown
<i>cysM</i>	8.129	putative O-acetylserine sulfhydrylase	Energy and Amino Acid Metabolism
<i>cysA</i>	5.460	serine O-acetyltransferase	Energy and Amino Acid Metabolism
<i>mtlF</i>	4.901	PTS system, mannitol-specific IIA component	Carbohydrate Metabolism, Transferases
<i>mtlD</i>	4.753	mannitol-1-phosphate 5-dehydrogenase	Carbohydrate Metabolism, Oxidoreductases
<i>CDR20291_1260</i>	4.374	putative membrane protein	Unknown
<i>mtlR</i>	3.886	mannitol operon transcriptional antiterminator	Transcription factors

<i>CDR20291_2627</i>	3.031	cytosine permease	Transporters
<i>mtlA</i>	2.984	PTS system, mannitol-specific IIBC component	Carbohydrate Metabolism, Transferases
<i>CDR20291_2626</i>	2.978	putative carbon-nitrogen hydrolase	Unknown
<i>CDR20291_0474</i>	2.623	putative exported protein	Unknown
<i>ribH</i>	2.430	6,7-dimethyl-8-ribityllumazine synthase (riboflavin synthase beta chain)	Metabolism of Cofactors and Vitamins, Transferases
<i>CDR20291_1593</i>	2.319	putative arsenical pump membrane protein	Unknown
<i>ribD</i>	2.232	diaminohydroxyphosphoribosylaminopyrimidine deaminase / 5-amino-6-(5-phosphoribosylamino) uracil reductase (riboflavin biosynthesis protein)	Metabolism of Cofactors and Vitamins, Cell Community, Oxidoreductases, Hydrolases
<i>fdhA</i>	2.185	L-seryl-tRNA (Ser) seleniumtransferase	Metabolism of Other Amino Acids, Translation, Transferases
<i>modA</i>	2.176	molybdate transport system substrate-binding protein	Membrane Transport, Transporters
<i>CDR20291_0182</i>	2.171	putative membrane-associated metalloprotease	Unknown
<i>CDR20291_2397</i>	2.167	TetR-family transcriptional regulator	Unknown
<i>CDR20291_0146</i>	2.153	putative riboflavin transporter	Unknown
<i>CDR20291_0178</i>	2.152	cyclopropane-fatty-acyl-phospholipid synthase	Unclassified Metabolism, Transferases
<i>CDR20291_2191</i>	2.145	putative pilin protein, general secretion pathway protein G	Membrane Transport, Secretion

			System
<i>CDR20291_1446</i>	2.124	prophage antirepressor-related protein	Unknown
<i>CDR20291_2012</i>	2.100	ABC-2 type transport system ATP-binding protein	Transporters
<i>CDR20291_1405</i>	2.089	putative polysaccharide deacetylase	Unknown
<i>ribB</i>	2.083	riboflavin synthase	Metabolism of Cofactors and Vitamins, Transferases
<i>CDR20291_0763</i>	2.073	aconitate hydratase	Carbohydrate Metabolism, Lyases
<i>glyA</i>	2.069	glycine hydroxymethyltransferase	Carbohydrate, Energy, Amino Acid, Other Amino Acid, and Cofactors and Vitamin Metabolism, Transferases
<i>iorB</i>	2.027	indolepyruvate ferredoxin oxidoreductase, beta subunit	Unclassified Metabolism, Oxidoreductases
<i>CDR20291_1816</i>	2.007	putative lipoprotein	Unknown
<i>CDR20291_0765</i>	2.001	MarR-family transcriptional regulator	Unknown
Down-regulated			
<i>nfo</i>	2.042	deoxyribonuclease IV	Replication and Repair, Hydrolases
<i>CDR20291_1819</i>	2.090	putative phage-related deoxycytidylate deaminase (putative late competence protein)	Nucleotide Metabolism, Secretion Systems, Hydrolases
<i>CDR20291_0177</i>	2.112	putative oxidoreductase, NAD / FAD binding subunit	Unknown
<i>CDR20291_3153</i>	2.114	type IV pilus assembly protein	Secretion Systems

<i>CDR20291_1319</i>	2.257	putative phage shock protein	Unknown
<i>CDR20291_1685</i>	2.274	putative exonuclease	Unknown
<i>CDR20291_0175</i>	2.333	anaerobic carbon-monoxide dehydrogenase catalytic subunit	Energy Metabolism, Xenobiotics biodegradation and Metabolism, Oxidoreductases
<i>CDR20291_2875</i>	2.424	conserved hypothetical protein	Unknown
<i>CDR20291_2931</i>	2.599	putative amino acid permease	Unknown
<i>CDR20291_2077</i>	3.005	putative sodium:dicarboxylate symporter	Unknown
<i>CDR20291_2932</i>	3.055	putative glutamine amidotransferase	Peptidases
<i>selD</i>	49.582	selenide, water dikinase	Metabolism of Other Amino Acids, Transferases

691

692 Figure Legends

693 Figure 1: Growth curves with complementing plasmid.

694 *C. difficile* R20291 pJS116 (wild-type, empty vector) (●), *C. difficile* KNM6 pJS116
695 ($\Delta selD$, empty vector) (■), and *C. difficile* KNM6 pKM142 ($\Delta selD::selD^+$, *pselD*) (▲)
696 were grown in TY medium at (A) 4% hydrogen and (B) 1.7% hydrogen and growth was
697 monitored over an 8 hour period. Data points represent the average from two
698 independent experiments and error bars represent the standard deviation from the
699 mean.

700 **Figure 2: Insertion by *C. difficile* CRISPR-Cas9 genome editing tool and the slight**
701 **growth defect of a *C. difficile* $\Delta seID$ strain.**

702 (A) Graphical representations of the three strains used in this study. Shown as a triangle
703 is the target site of the gRNA and the line indicates the site of the deletion. (B) DNA was
704 isolated from *C. difficile* R20291 (wild-type), KNM6 ($\Delta seID$), and KNM9 ($(\Delta seID::seID^+)$).
705 The region surrounding the *seID* gene was amplified from the chromosome, and the
706 resulting DNA was separated on an agarose gel. A clean deletion of *seID* is indicated by
707 a faster-migrating DNA band while wild-type and the insertion mutation (restoration) is
708 indicated by a slower-migrating DNA band. (C-D) *C. difficile* R20291 (wild-type) (●), *C.*
709 *difficile* KNM6 ($\Delta seID$) (■), and *C. difficile* KNM9 ($\Delta seID::seID^+$) (▲) were grown in (C)
710 BHIS medium and (D) TY medium at 1.7% hydrogen and growth was monitored over a
711 24 hour period. Data points represent the average from three independent experiments
712 and error bars represent the standard deviation from the mean.

713 **Figure 3: Selenoproteins do not have an effect on germination of *C. difficile***
714 **R20291 spores.**

715 Purified *C. difficile* R20291 (wild-type) (●/○), *C. difficile* KNM6 ($\Delta seID$) (■/□), and *C.*
716 *difficile* KNM9 ($\Delta seID::seID^+$) (▲/△) spores were suspended in (A) BHIS or (B) TY
717 medium supplemented with 10 mM taurocholate (open symbols) or without taurocholate
718 (closed symbols). The change in OD₆₀₀ during germination was measured over time at
719 37°C. The data represents the average of three biological replicates and error bars
720 represent the standard deviation from the mean.

721 **Figure 4: *seID* plays a role in outgrowth of *C. difficile* R20291 spores.**

722 Purified *C. difficile* R20291 (wild-type) (●), *C. difficile* KNM6 ($\Delta seID$) (■), and *C. difficile*
723 KNM9 ($\Delta seID::seID^+$) (▲) spores were germinated and then resuspended in (A) BHIS or
724 (B) TY medium, and the OD₆₀₀ was measured over an 8 hour period and then again at
725 24 hours. Data points represent the average from three independent experiments and
726 error bars represent the standard deviation from the mean.

727 **Figure 5: Distribution of functions of up- and down-regulated genes from RNA-**
728 **seq.**

729 Pie charts of the KEGG functional pathways of genes which were (A) up-regulated and
730 (B) down-regulated from RNA-seq analysis. Percentages of each function are shown in
731 the legends.

732 **Figure 6: Fold change of transcript levels in *C. difficile* KNM6 ($\Delta seID$) compared to**
733 ***C. difficile* R20291**

734 RNA was extracted from *C. difficile* R20291 and KNM6 ($\Delta seID$) strains grown to an
735 OD₆₀₀ of 0.6 in TYG medium, DNA was depleted, and cDNA was synthesized.
736 Quantitative reverse transcription-PCR was performed to determine the fold change of
737 transcript levels in the KNM6 ($\Delta seID$) strain compared to wild-type R20291 strain at
738 each 4% and 1.7% hydrogen levels. Fold change for the following genes are shown: (A)
739 *CDR20291_0962*, (B) *CDR20291_0963*, (C) *mtlF*, (D) *prdB*, (E) *grdB*, (F)
740 *CDR20291_2627*, and (G) *CDR20291_2932*. Data represents the average from three
741 independent experiments run in technical triplicate and error bars represent the
742 standard deviation from the mean. Technical replicate outliers were excluded.

743

744 **Supplemental Information Legend**

745 Figure S1: Growth curve in TYG

746 Figure S2: Deletion of *spo0A* in *C. difficile* R20291

747 Table S1: Complete list of gene expression fold-change from RNA-seq of wild-type and
748 *se/D* mutant strains.

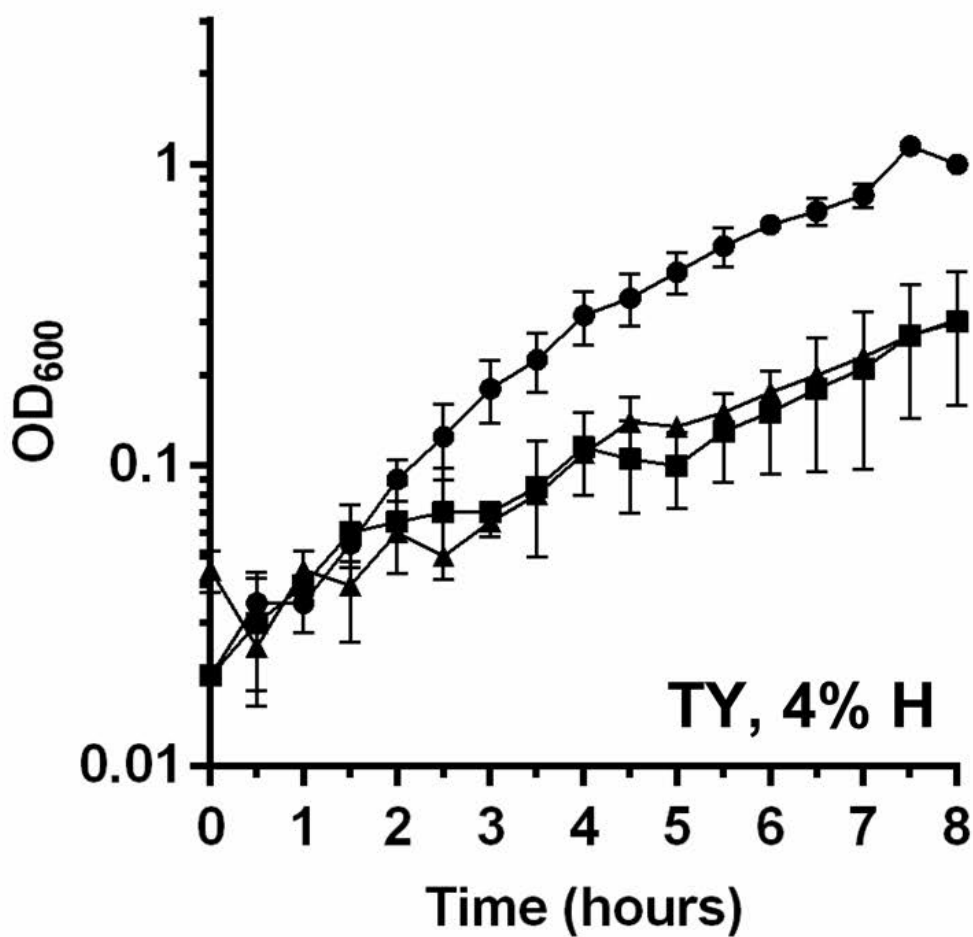
749 Table S2: Strains and plasmids used in this study.

750 Table S3: Oligonucleotides used in this study.

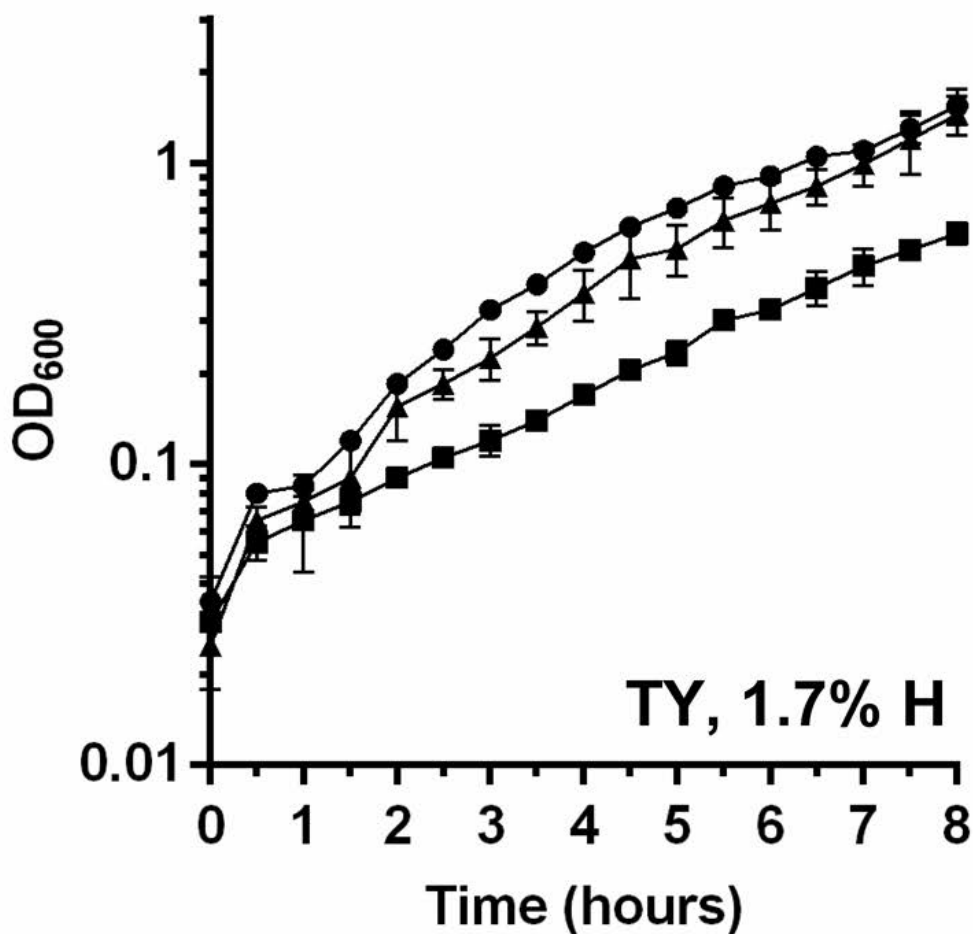
751

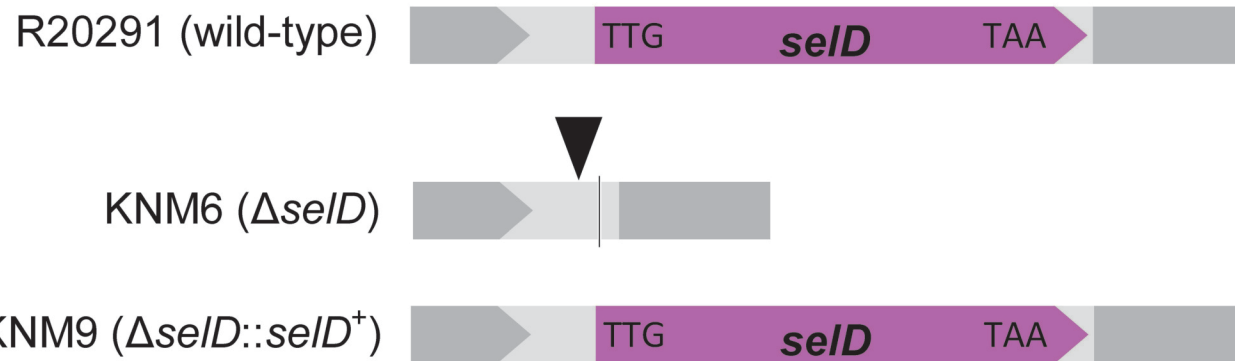
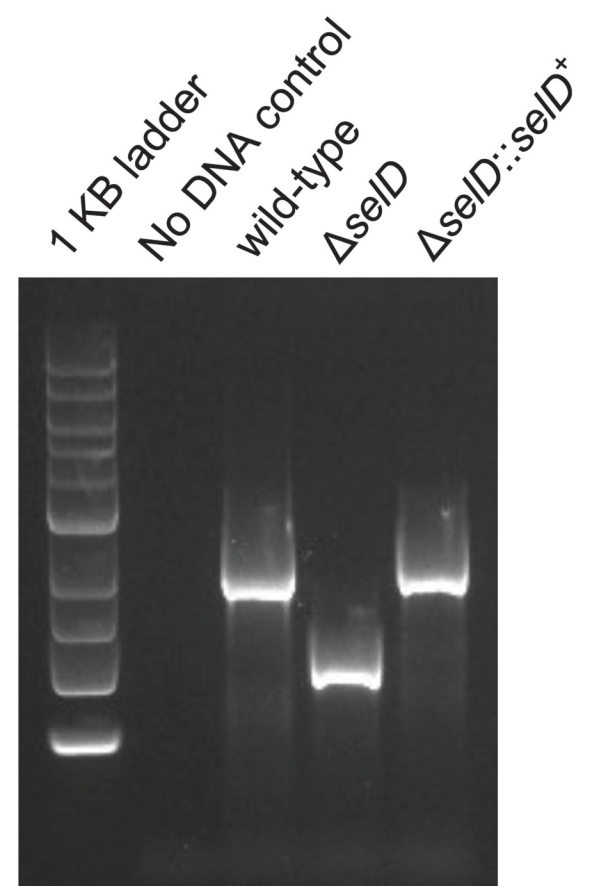
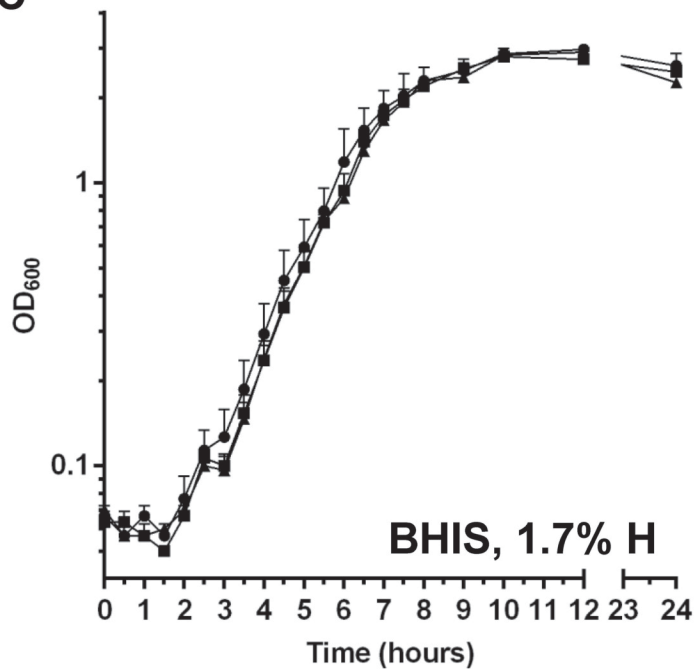
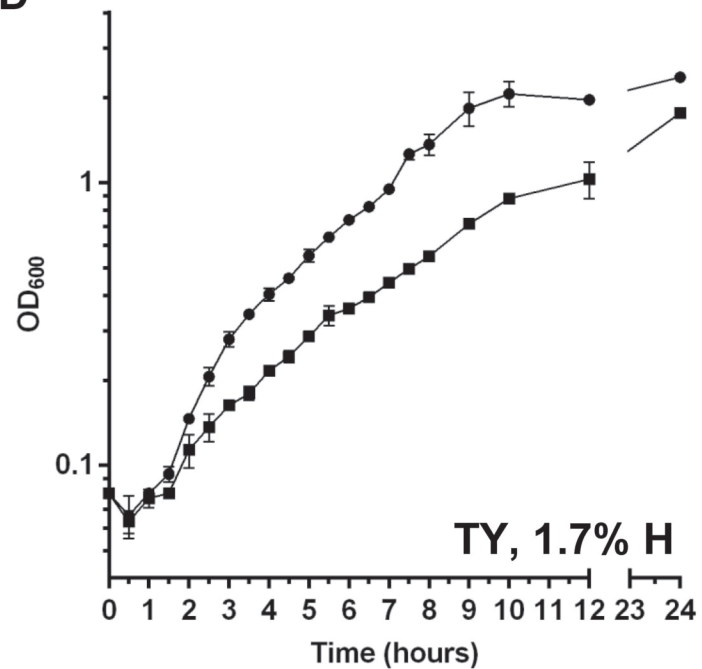
752

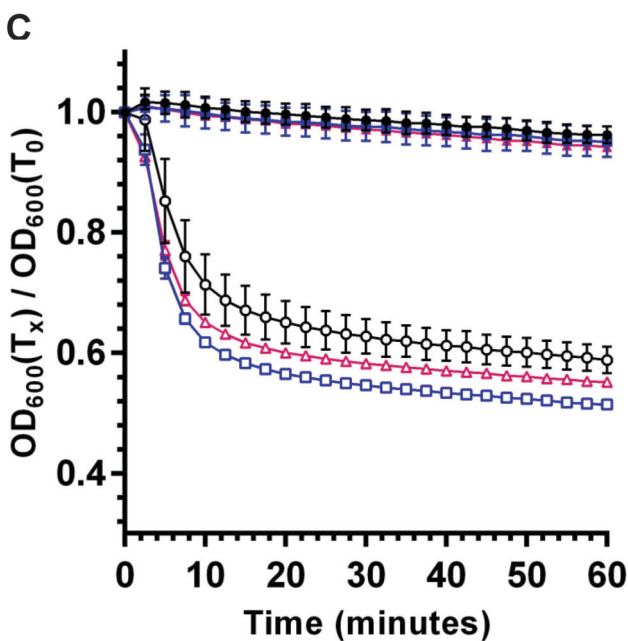
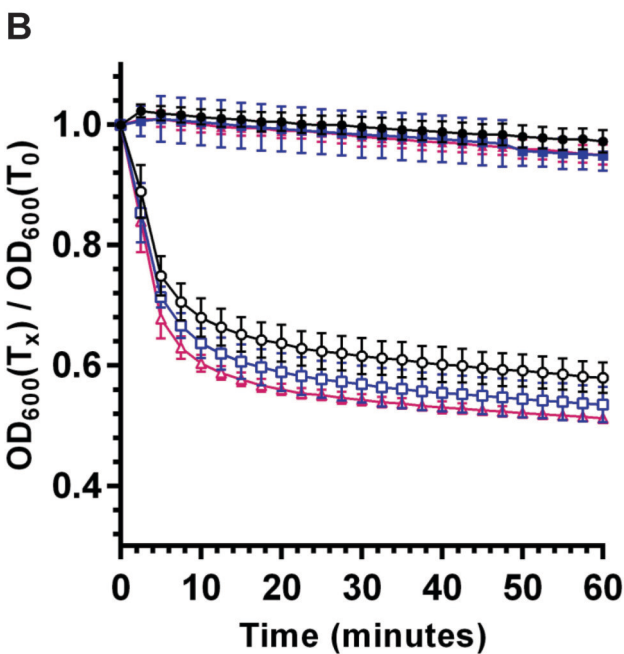
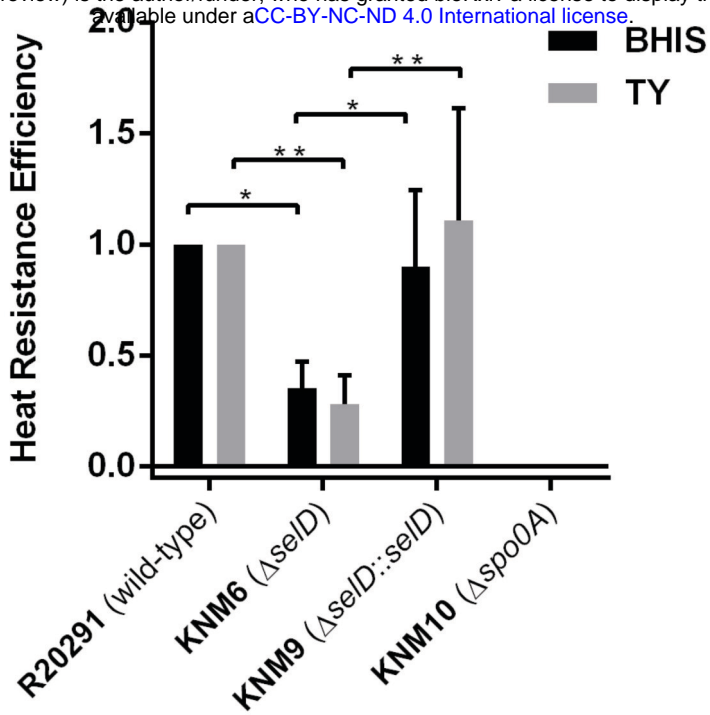
A



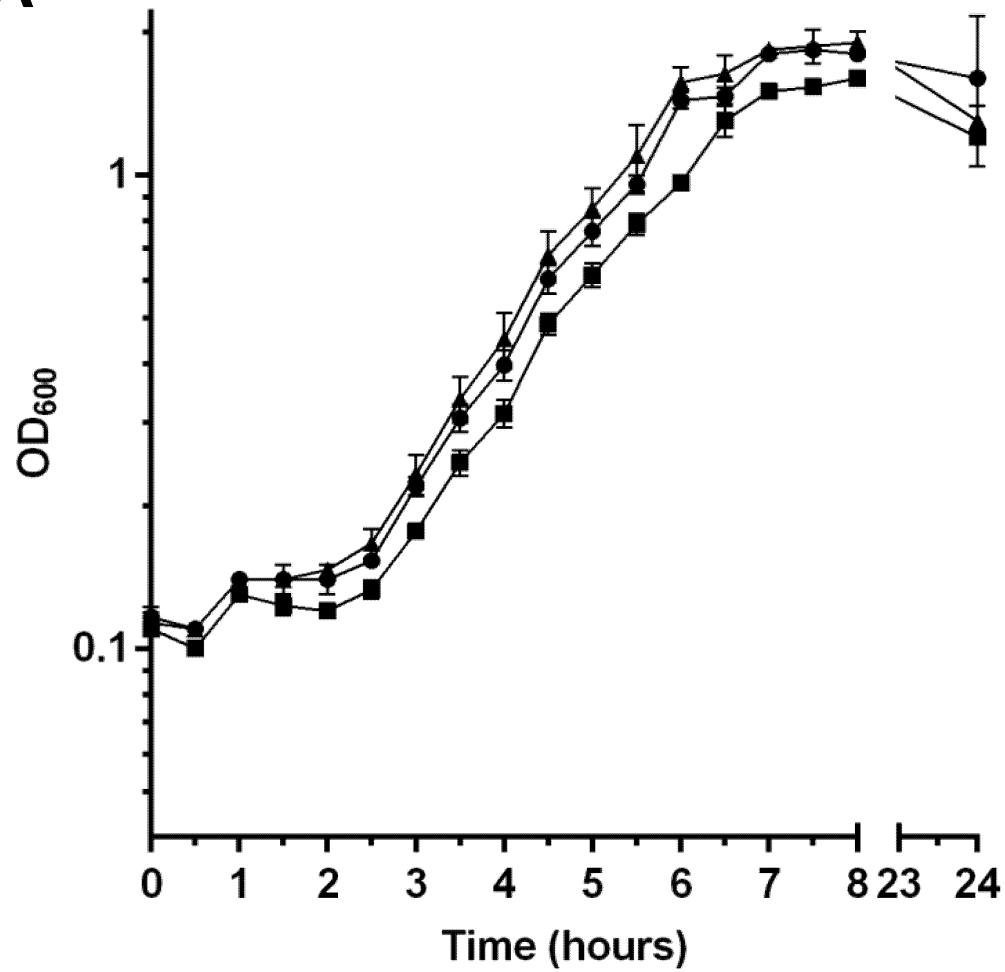
B



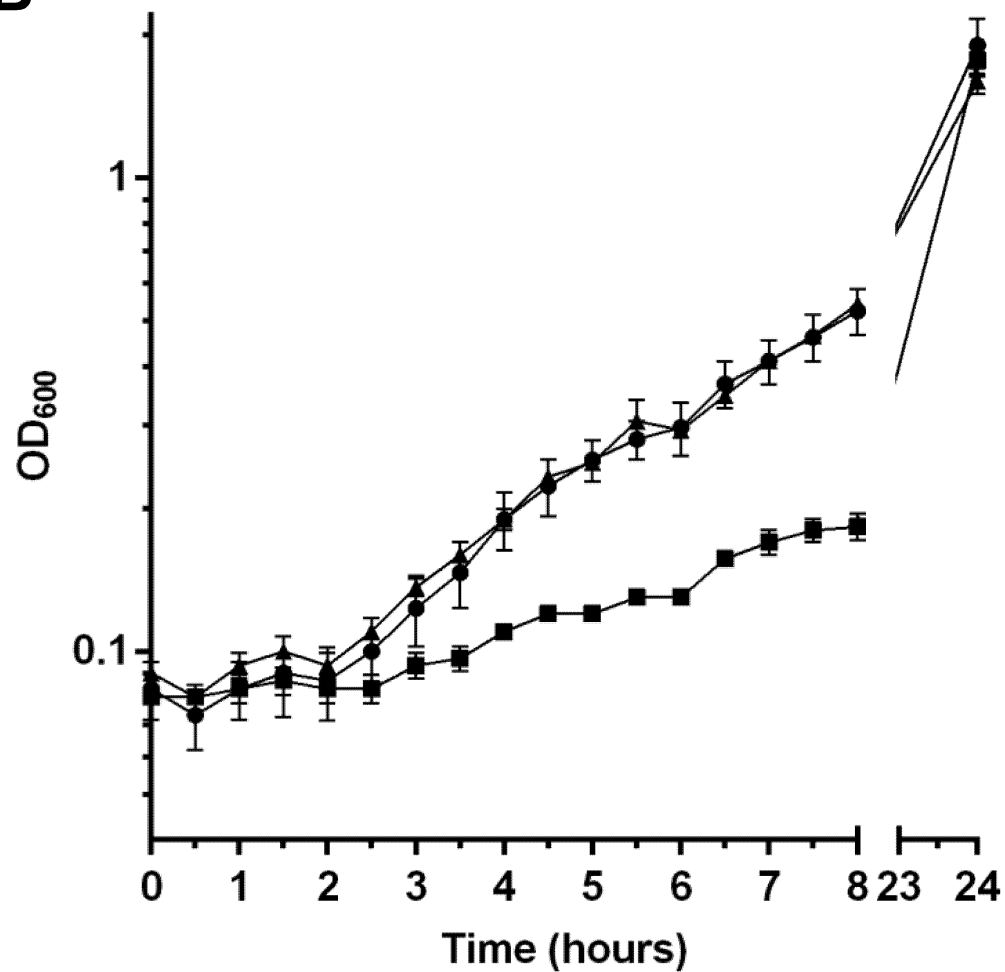
A**B****C****D**

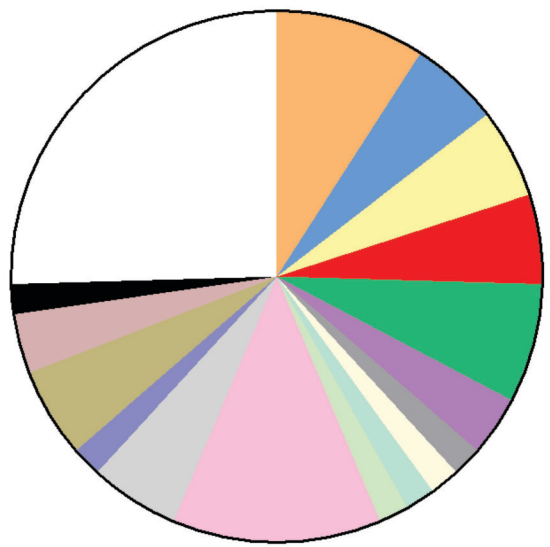


A

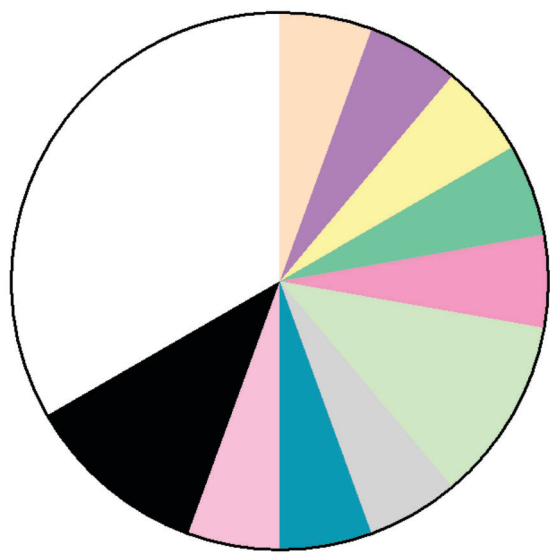


B

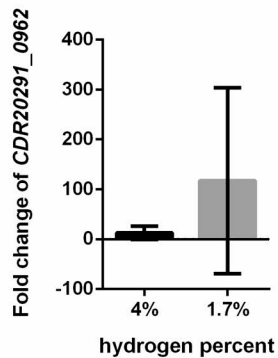
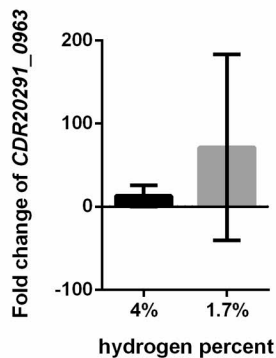
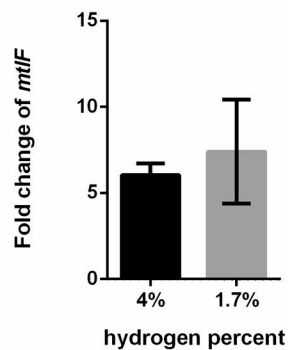
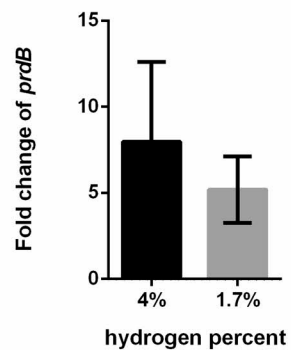
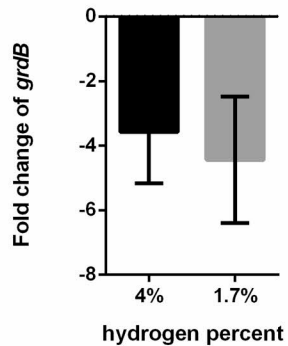
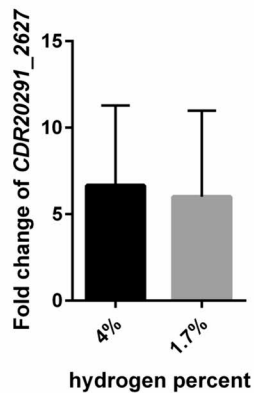
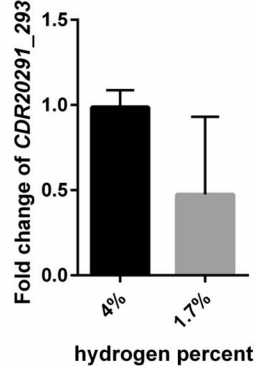


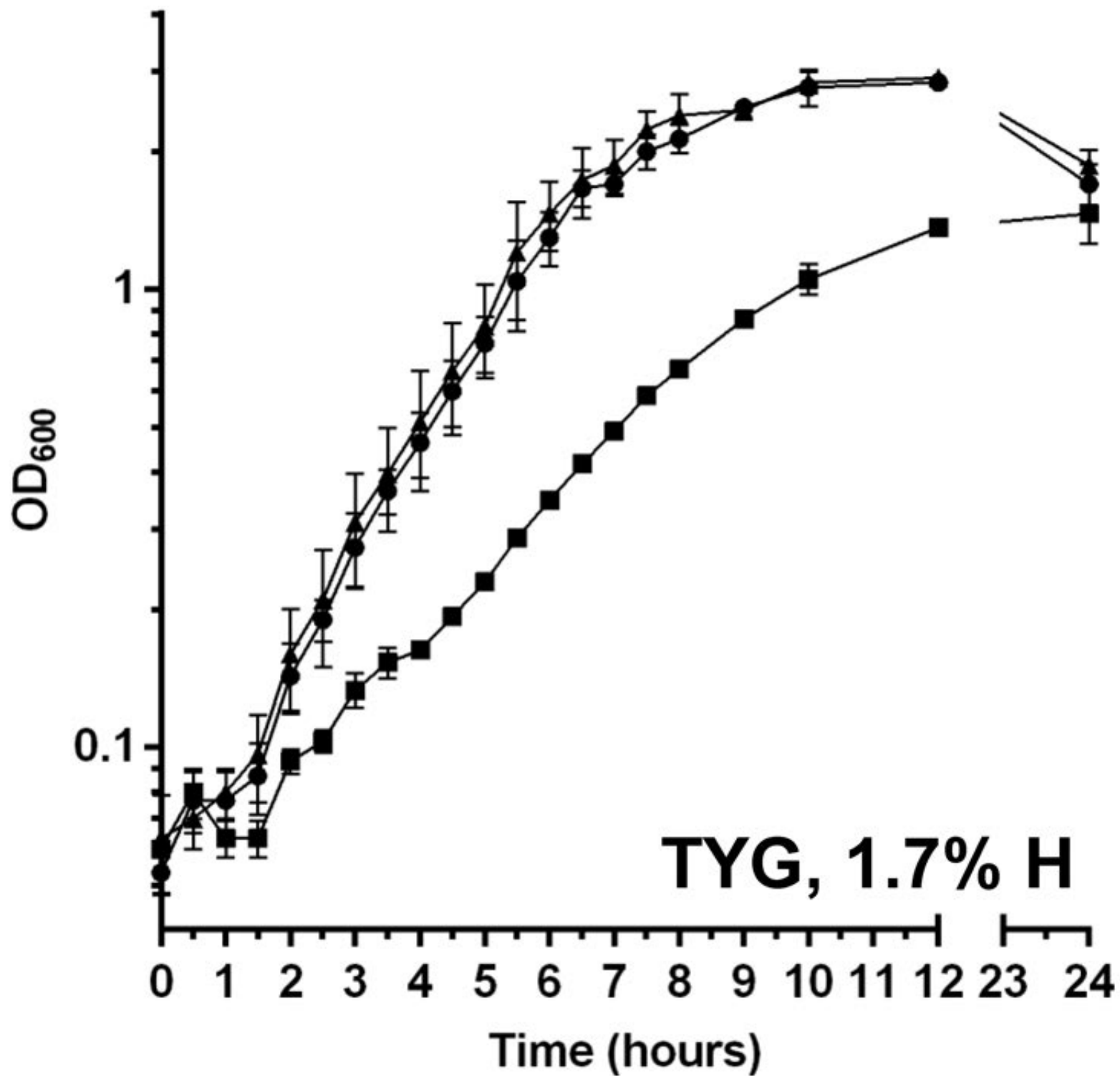
A**Up-regulated**

- 9.09% Carbohydrate Metabolism
- 5.45% Unclassified Metabolism
- 5.45% Energy Metabolism
- 5.45% Amino Acid Metabolism
- 7.27% Cofactors and Vitamins Metabolism
- 3.64% Other Amino Acid Metabolism
- 1.82% Translation
- 1.82% Transcription Factors
- 1.82% Cell Community
- 1.82% Hydrolases
- 12.73% Transferases
- 5.45% Oxidoreductases
- 1.82% Lyases
- 5.45% Transporters
- 3.64% Membrane Transport
- 1.82% Secretion System
- 25.45% Unknown

B**Down-regulated**

- 5.56% Nucleotide Metabolism
- 5.56% Other Amino Acid Metabolism
- 5.56% Energy Metabolism
- 5.56% Xenobiotics Biodegradation and Metabolism
- 5.56% Replication and Repair
- 11.11% Hydrolases
- 5.56% Oxidoreductases
- 5.56% Peptidases
- 5.56% Transferases
- 11.11% Secretion System
- 33.33% Unknown

A**B****C****D****E****F****G**



7 KB ladder

No DNA control

wild-type

Δ spo0A

